



Univerzita Komenského v Bratislave  
Fakulta matematiky, fyziky a informatiky



**Ing. Matúš Sedlák**

**Autoreferát dizertačnej práce**

**Gamma-ray and conversion-electron spectroscopy at CERN-ISOLDE facility  
(Spektroskopia gamma žiarenia a konverzných elektrónov na zariadení CERN-  
ISOLDE)**

**na získanie akademického titulu philosophiae doctor**

**v odbore doktorandského štúdia:  
4.1.5. Jadrová a subjadrová fyzika**

**Bratislava 30.4.2019**

**Dizertačná práca bola vypracovaná v dennej forme doktorandského štúdia  
na Fyzikálnom ústave Slovenskej akadémie vied**

**Predkladateľ:**           **Ing. Matúš Sedlák**  
Oddelenie jadrovej fyziky  
Fyzikálny ústav SAV  
Dúbravská cesta 9,  
845 11, Bratislava

**Školiteľ:**               **Mgr. Martin Venhart, PhD.**  
Oddelenie jadrovej fyziky  
Fyzikálny ústav SAV  
Dúbravská cesta 9,  
845 11, Bratislava

**Študijný odbor:** 4.1.5. Jadrová a subjadrová fyzika

**Predseda odborovej komisie:**

prof. RNDr. Jozef Masarik, DrSc.  
Fakulta matematiky, fyziky a informatiky UK  
Mlynská dolina,  
842 48, Bratislava

## Abstrakt

Témou práce je systematické štúdium tvarovej koexistencie nepárnych izotopov zlata v oblasti s neutrónovým číslom  $N=104$ . Experimentálna časť tejto práce sa opiera o realizáciu experimentu IS521 na zariadení ISOLDE. Excitované stavy izotopov  $^{181,183}\text{Au}$  boli populované  $\beta^+/\text{EC}$  premenou  $^{181,183}\text{Hg}$  prekursorov, ktoré boli dodané zariadením ISOLDE. Jadrová štruktúra izotopov  $^{181,183}\text{Au}$  bola študovaná pomocou simultánnej spektroskopie konverzných elektrónov a  $\gamma$  kvánt. TATRA spektrometer, ktorý obsahuje unikátny páskový transportný systém založený na amorfnej kovovej páske, bol vyvinutý a úspešne použitý. Nový Broad Energy Germanium (BEGe) detektor bol použitý v experimente v oblasti základného výskumu jadrovej štruktúry po prvýkrát. Tento detektor má výborné rozlíšenie, spojitú pozadie a takmer ideálne tvarované píky podobné Gaussovému rozdeleniu, čo umožňuje lepšie rozoznanie pík v multipletoch a určenie energie pík s presnosťou na 30 eV. Vďaka tejto presnosti mohol byť použitý kombinačný princíp, ktorý navrhli Rydberg a Ritz, na zostavovanie rozpadových schém. Pri štúdiu nuklidov s nepárnym hmotnostným číslom často čelíme spektrám, ktoré sa vyznačujú veľkou hustotou pík. Preto bola použitá inovatívna metóda na separáciu pôvodnej premeny od dcérskych premien v spektrách. Rozpadová schéma nuklidu  $^{183}\text{Au}$  bola značne doplnená a opravená oproti tej v predošlej štúdiu a rozpadová schéma pre nuklid  $^{181}\text{Au}$  bola skonštruovaná po prvýkrát. Boli doplnené systematiky niektorých stavov a mierna zmena tvaru bola identifikovaná pomocou ich porovnania s PTRM výpočtami. Hlavným výsledkom práce je pozorovanie parabolického trendu v systematike vnorených (intruder) stavov s minimom presne medzi dvoma neutrónovými uzavretými vrstvami,  $N=104$ , čo zodpovedá izotopu  $^{183}\text{Au}$ .

## Abstract

The topic of this thesis is the systematic study of the shape coexistence in odd-mass Au isotopes in the vicinity of  $N=104$  mid-shell point. Experimental part of the thesis was performed at ISOLDE facility, within the scope of the IS521 experiment. Excited states of  $^{181,183}\text{Au}$  isotopes were populated by  $\beta^+/\text{EC}$  decay of  $^{181,183}\text{Hg}$  precursors produced by ISOLDE. Nuclear structure of  $^{181,183}\text{Au}$  isotopes was investigated by means of simultaneous spectroscopy of conversion electrons and  $\gamma$  rays. A unique tape transportation system TATRA, based on rapidly quenched metallic tape, was designed and successfully commissioned. For the first time in the fundamental nuclear structure experiment, novel Broad Energy Germanium (BEGe) detector was used. Its supreme energy resolution, together with almost ideally Gaussian peak shape allowed peak recognitions in many multiplets and the determination of peak energies with 30 eV precision. It was so precise, that Rydberg-Ritz combination principle was used for level scheme constructions. An enormous complexity of measured spectra emerges in the case of odd-mass nuclei study. Therefore, innovative method was developed. Results of the study are significantly improved level scheme of the  $^{183}\text{Au}$  in comparison with previous work and the level scheme of the  $^{181}\text{Au}$  was constructed for the first time. Systematics of particular states of odd-Au isotopes were extended and slight change in shape based on PTRM calculations was observed. The key result is observation of a parabolic trend in the systematics of intruder states with its minimum in neutron

midshell point  $N = 104$  ( $^{183}\text{Au}$ ).

## Introduction

The atomic nucleus, discovered by Ernest Rutherford in 1911 by interpretation of the famous gold-foil experiment [1] performed by Hans Geiger and Ernest Marsden, represents one of the fundamental building blocks of the matter in the Universe. It takes place between atoms and the hadrons in a chain of basic constituents, which stretches from quarks to galaxies. In common with many of its neighbours in the chain, the basic problem of nuclear structure physics is a quantum many-body one. Therefore, nuclear physics continues to be one of the most fascinating fields in a fundamental science. Nucleus generally consists of a large finite number of nucleons (neutrons and protons) interacting via a strong short-range force. The precise form of this effective interaction is still not known. In a sense, its determination is one of the fundamental goals of nuclear physics. The route, towards this goal, involves systematic predictions and domains testing of its applicability of the current models by probing excited states of nuclei in a great detail.

Important feature related to the nuclear structure is the shape coexistence, i.e., observation of differently shaped excited states (eigenstates) in particular atomic nucleus. The shape coexistence is known as a feature of nuclei over 50 years with three extensive reviews published [2–4].

This thesis deals with the systematic study of the shape coexistence in odd-Au isotopes in the vicinity of  $N = 104$  mid-shell point. Odd-mass isotopes in general herald the unique systems for nuclear structure studies, where the odd particle (proton or neutron) acts as a probe of the even-even core and yields information on independent particle states, of deformation (both axial and triaxial shapes), on pairing (from the blocking effect), on rotational collectivity, and on identification of intruder states almost free of mixing. The coupling of independent particle states with core excitations lead to high level density at low energies in odd-mass nuclei. Moreover, unlike in even-even nuclei, the decay schemes involve multiple paths to the ground states and multipolarities of transitions are dominated by  $M1$  and mixed  $M1 + E2$ . This is reflected in an enormous complexity of measured spectra, both for  $\gamma$  rays and conversion electrons. Therefore, an excellent energy resolution is critical parameter. To achieve acceptable conditions, innovative methods needed to be developed to study odd-mass nuclei.

Experimental part of the thesis was performed at ISOLDE facility, within the scope of the IS521 experiment [5]. Excited states of  $^{181,183}\text{Au}$  isotopes were populated by  $\beta^+/\text{EC}$  decay of  $^{181,183}\text{Hg}$  precursors produced by ISOLDE. Nuclear structure of  $^{181,183}\text{Au}$  isotopes was investigated by means of simultaneous spectroscopy of conversion electrons and  $\gamma$  rays. A unique tape transportation system TATRA, based on rapidly quenched metallic tape, was designed and successfully commissioned. For the first time in the fundamental nuclear structure experiment, novel Broad Energy Germanium (BEGe) detector was used. Its supreme energy resolution, together with almost ideally Gaussian peak shape allowed peak recognitions in many multiplets and the determination of peak energies with 30 eV precision. It was so precise, that Rydberg-Ritz combination principle [6] was used for level scheme constructions.

Decay scheme of  $^{183}\text{Hg}$  was significantly improved [7] in comparison with previous work [8]. Decay scheme of  $^{181}\text{Hg}$  was constructed for the first time.

## Experiment IS521

The CERN-based experiment IS521 (spokesperson: Martin Venhart) has been proposed to study excitation states in neutron deficient odd-Au by simultaneous detection of X-rays,  $\gamma$  rays and conversion electrons [5]. The excited states of odd-Au isotopes were populated by the  $\beta^+$ /EC decay of corresponding Hg isotopes. This study leads to better understanding of nuclear structure and low-energy shape coexistence in the neutron mid-shell region in odd-Au isotopes. The first part of the IS521 experiment was carried out in August 2014 and the second one in August 2016.

A molten lead was used as the ISOLDE target, which was irradiated with the pulsed proton beam delivered by the Proton-Synchrotron Booster. A plasma ion source was used for ionisation of isotopes, residuals of nuclear reactions inside the target. These isotopes were extracted with the extracting voltage of 30 kV and then mass separated using the General Purpose Separator adjusted for required mass number. Elements in the region from Hf to Pt were not extracted from the target, because they are refractory metals. Production and extraction of Pb, Tl and Au was very low, therefore practically pure beam of Hg ions was delivered to the LA1 beamline for travelling experimental setups, where the TATRA spectrometer was installed. A radioactive sample was created by deposition of the Hg beam on the metallic tape of the TATRA's tape transportation system. The sample with sufficient collected activity was transported to the measurement position while the beam gate was closed. This is periodically repeated according to the half-life of the measured isotope. Two separate runs were performed with different detectors coupled to the TATRA system.

## TATRA spectrometer

TATRA [9] is compact spectrometer, which was developed and constructed at the Institute of Physics, Slovak Academy of Sciences in Bratislava, Slovakia. The name, TATRA, is an abbreviation of the TApe TRANsportation system and also evokes the origin of the system (TATRA Mountains are the highest mountain range in Slovakia).

The spectrometer is composed of a vacuum chamber with the tape transportation system inside, detector of electrons coupled with it and several  $\gamma$  detectors outside, which can be of any type. Its primary purpose are nuclear structure studies, thanks to its capability of measuring  $\gamma$  rays and conversion electrons simultaneously.

TATRA spectrometer has been under development since 2011 and the first use of it was during the first run of the experiment IS521 at the ISOLDE facility in 2014. In that time we were unable to properly measure low-energy  $\gamma$  rays and X-rays, because the measurement point was positioned inside the tube from stainless steel with 2 mm wall thickness. Another problem was non-functioning silicon detector with wrong type of the preamplifier, and therefore no electron data were obtained. Later, the detector was repaired under warranty by the manufacturer and TATRA spectrometer was modified for the better low-energy photons transmission. The measurement point has been moved closer to the main vacuum chamber and it was positioned to the centre of aluminium cube with four 50  $\mu\text{m}$  thin titanium foil windows. Modified TATRA spectrometer was successfully used during the second run of the experiment IS521 in 2016 at the ISOLDE facility. X-rays,  $\gamma$  rays and conversion electrons were measured with the spectrometer.

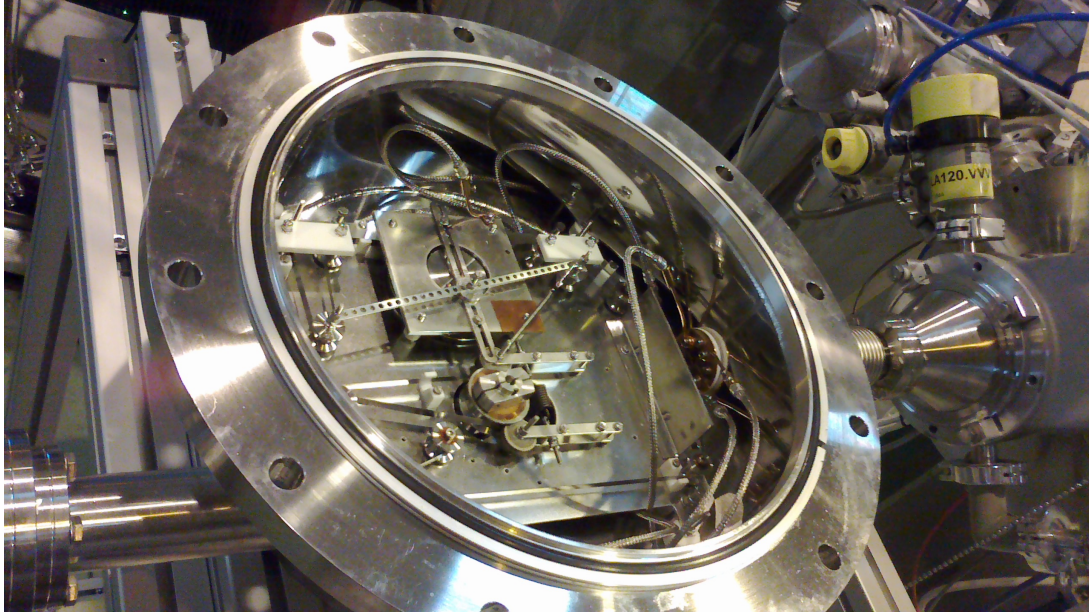


Figure 1: Photograph of opened TATRA chamber with the tape system inside. The chamber is connected to the LA1 beamline in the experimental hall of ISOLDE.

### **Tape transportation system**

The tape transportation system is the main component of TATRA spectrometer and its aim is collection and transportation of radioactive samples from the collection point to the measurement point. Samples of radioactive isotopes are produced by a deposition of a radioactive ion beam onto the metallic tape. The sample is transported into the measurement point right after the ion collection by a swift tape move. Since the sample is radioactive, the activity of studied isotope is continuously decreasing, while activities of daughter isotopes are increasing. When significant fraction of the sample decayed, a new one has to be delivered to the measurement point and the whole procedure is repeated periodically. Collection (ion deposition), transportation and measurement times depend on the half-life of the studied isotope and the yield of radioactive ion beam.

The tape length can be from 3 m to 80 m, while the accuracy in the tape move is better than 0.5 mm. The stepper motor has 200 main steps/rev with an option of a microstepping (3200 steps/rev in our case). The distance between the place of deposition and the measurement point is approximately 67 cm. The sample can be moved by this distance in less than 0.7 s. Its real photograph of the system at LA1 beamline is shown in Fig. 1.

### **Detectors**

Presently the TATRA spectrometer has capability to place four detectors around the measurement point of any type and one detector can be placed in the front of the sample inside the vacuum chamber. In the case of IS521 experiment, Ge detectors were used for  $\gamma$ -ray detection and one Si(Li) detector located inside the vacuum chamber was used for the measurement of electrons. Real photograph of this system from the second run of IS521 experiment is given in Fig. 2.



Figure 2: Photograph of TATRA spectrometer at ISOLDE LA1 beamline with all detectors mounted.

### Electronics

IS521 experiment would not be successful without used custom electronics like custom signal converter for Si(Li) detector and GO-box. The GO-box is an array of linear amplifiers with the gain of 2, 4 or 8. Each channel has an option of the offset correction and SMA connectors for the input and the output. This amplifier array is constructed like stand-alone unit packeted in the box with its own power supply and it has been designed at the University of Liverpool. GO-box is connected between preamp and DAQ system.

Another piece of custom electronics used in TATRA system is the transistor reset type of preamplifier (TRP) to RC feedback (RCFB) signal converter. There is need of signal converting because the XIA Pixie-16 DGF module accepts only unipolar signal with exponential decay to the baseline and amplitude up to 2.2 V, which is common for the  $\gamma$ -ray detector's preamplifier with RCFB. Our Si(Li) detector has the integrated

TRP and cannot be replaced. For that reason I have developed an electric circuit capable of transforming the stairs like signal to signal with the exponential decay to the baseline. The converter circuit was designed as two sided printed circuit board (PCB). The converter circuit PCB was placed inside the blank NIM module and it uses the power supply of the NIM crate. Inputs and outputs are BNC connectors located on the front panel of the NIM module together with the potentiometer for gain control.

## Summary of experimental results and discussion

### $^{183}\text{Hg}$ decay

The results in this section are published in [7, 10]. The half-life of  $^{183}\text{Hg}$  is  $9.4(7)$  s [11] and the  $\beta$ -decay energy is  $6385(12)$  keV [12]. Total absorption experiment shown that a large concentration of  $\beta$ -decay strength to states in  $^{183}\text{Au}$  in the excitation energy range from 1600 keV to 1900 keV [13]. Analysis of the IS521 data, presented here, revealed that, a single state at 1682.30 keV excitation energy appears to be very strongly fed by  $\beta^+$ /EC decay of the  $^{183}\text{Hg}$ . This suggests its spin and parity of  $1/2^-$  or  $3/2^-$ , since the ground state of the  $^{183}\text{Hg}$  is  $1/2^-$  [14] and for  $^{183}\text{Au}$  ground state it is  $5/2^-$  [15]. This state appeared to be critical to elucidate the structure of  $^{183}\text{Au}$  isotope, see discussion later.

The focus of this study is to extend systematics of the energies of the lowest-lying

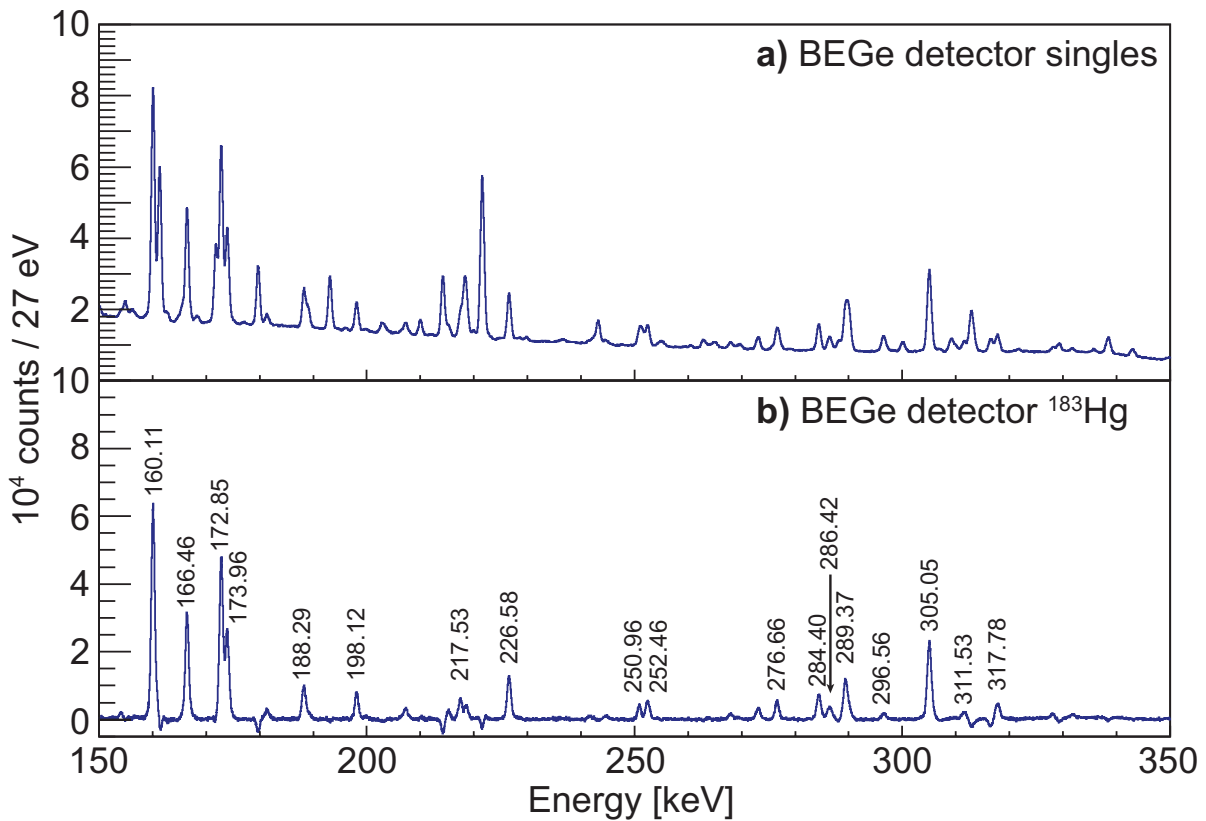


Figure 3: Singles  $\gamma$ -ray spectra measured with BEGe detector. (a) is total singles spectrum and (b) is singles spectrum assigned to the  $^{183}\text{Hg}$  decay. Figure is published in [7].



$1h_{9/2}$  and  $2f_{7/2}$  intruder states in  $^{183}\text{Au}$  relative to the non-intruder  $2d_{3/2} \oplus 3s_{1/2}$  states. This was carried out in systematic studies in the heavier odd-mass Au isotopes. Excited states at very low excitation energy ( $< 50$  keV) are common in odd-mass Au isotopes in this mass region, which make a level scheme construction more difficult. For identification of these states in  $^{183}\text{Au}$ , many deexcitation paths of the 1682.30 keV state were used with combination of high precision  $\gamma$ -ray spectroscopy by employing BEGe detector at high gain.

Innovative method was used to to spectra separation for both conversion-electron and  $\gamma$ -ray data. A comparison of total singles (a) and deconvoluted  $^{183}\text{Hg}$  decay singles spectra (b) measured with BEGe detector is in Fig. 3, and measured with Si(Li) detector is in Fig. 4.

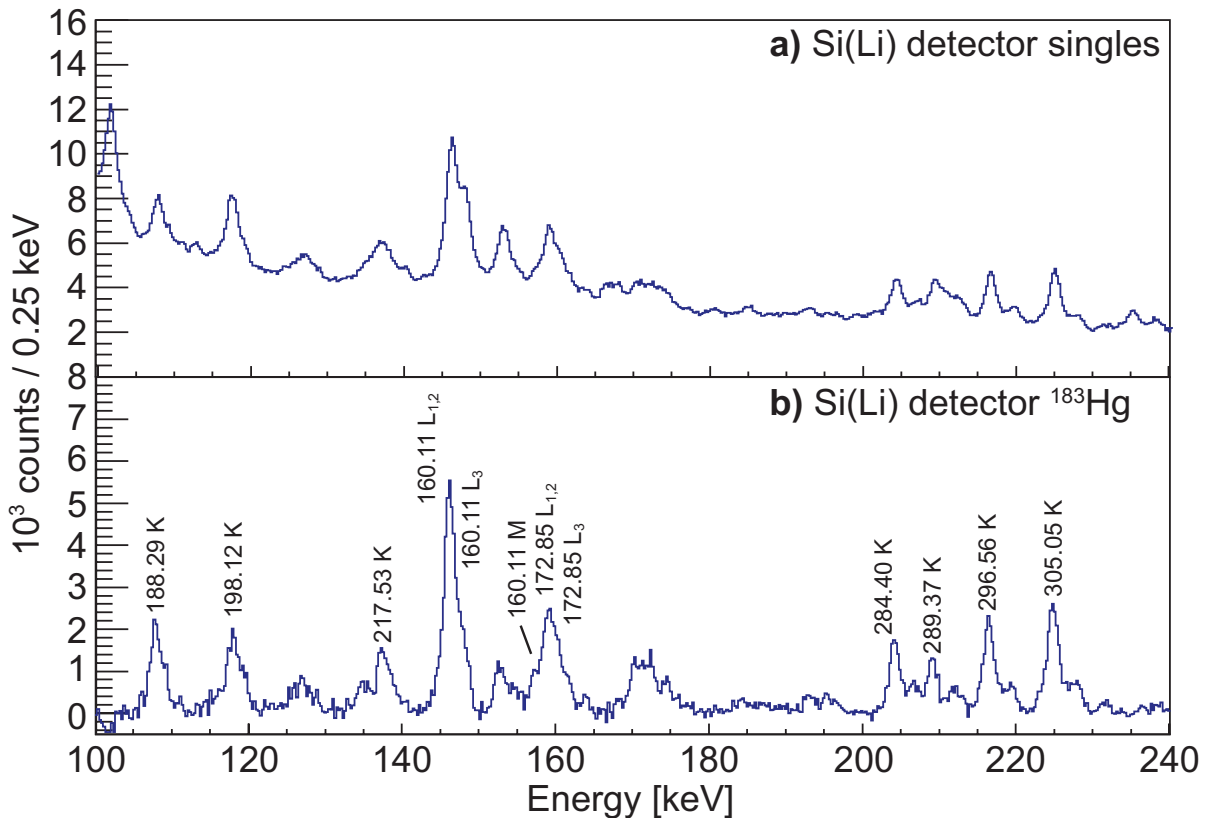


Figure 4: Electron singles spectra detected with the Si(Li) detector. (a) is total singles spectrum and (b) is single spectrum assigned to the  $^{183}\text{Hg}$  decay. Figure is published in [7].

Multipolarities of transitions assigned to the decay of  $^{183}\text{Au}$  were determined by comparison of experimental values with BrIcc [16] calculated values of internal conversion coefficients.

The level schemes of  $^{183}\text{Au}$  were constructed on the basis of  $\gamma$ - $\gamma$ -ray coincidences in conjunction with the Rydberg–Ritz combination principle. Coincidences of  $\gamma$  rays with conversion electrons were investigated separately. However, only a few coincidence gates of conversion electrons with sufficient statistical quality could be produced due to limited running time. The partial level scheme of low-lying negative-parity states associated with  $1h_{9/2}$  and  $2f_{7/2}$  intruder configurations that are fed by deexcitation of the 1682.30 keV level is given in Fig. 5. The partial level scheme of low-lying positive-parity states associated with the  $2d_{3/2} \oplus 3s_{1/2}$  proton–hole configurations, which is also

fed by deexcitation of the 1682.30 keV level is given in Fig. 6.

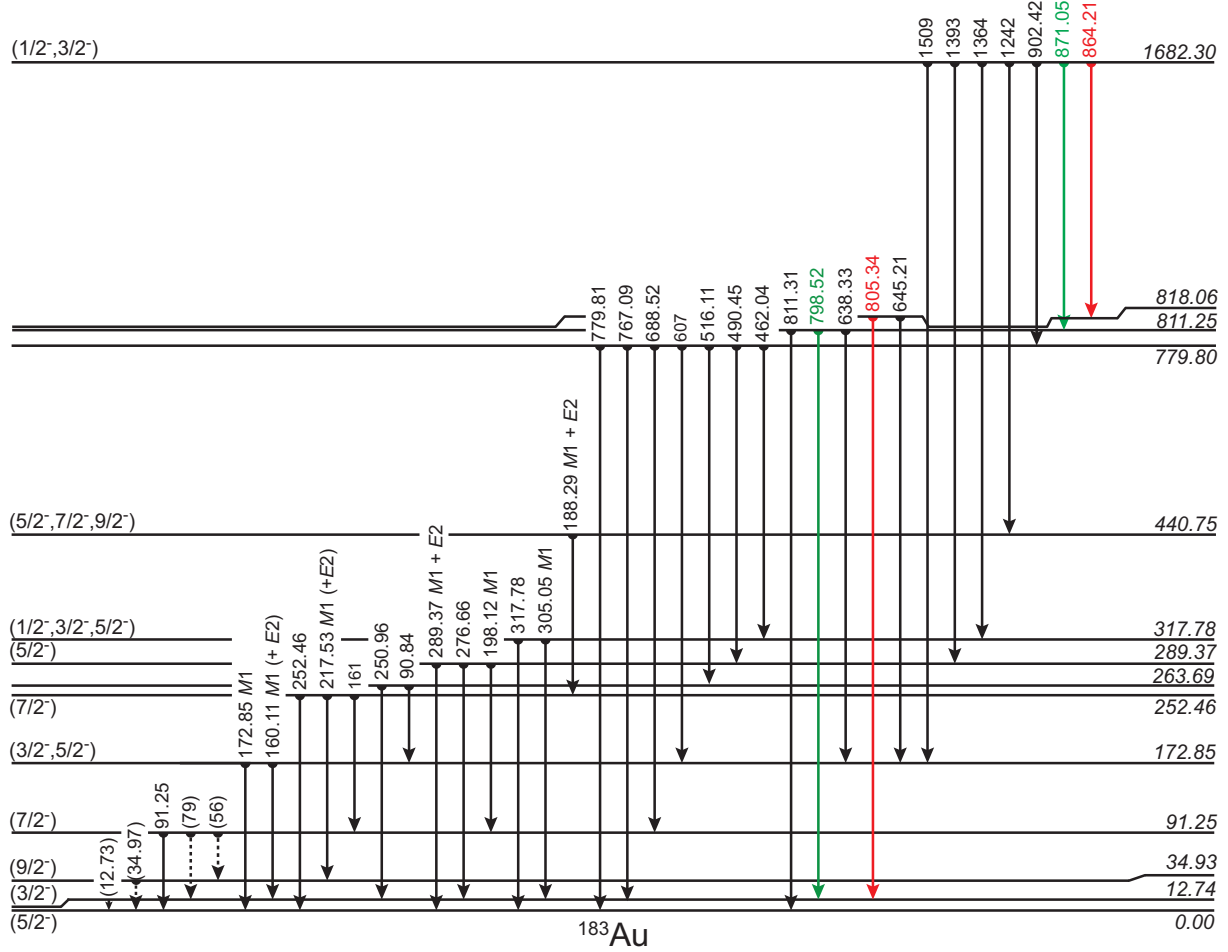


Figure 5: Partial level scheme of low-lying, negative-parity states associated with the  $1h_{9/2}$  and  $2f_{7/2}$  intruder configurations in the  $^{183}\text{Au}$  isotope deduced from the present work [7]. Transition energies were determined using the  $\gamma$ -ray singles spectrum detected with the BEGe detector. Transitions with energies given as integer numbers are either weak, dominated by other  $\gamma$  lines, or their energy exceeds 980 keV, which was the upper limit for the BEGe detector in this experiment, see the text for details. Their location in the scheme is proved by the  $\gamma$ - $\gamma$  coincidences. All states are populated via the decay of the 1682.30 keV state. Decay path used for the localisation of the critical 60.73 keV transition connecting intruder and proton-hole states are highlighted with red colour.

The 1682.30 keV state can be used to determine the energy difference between intruder and “normal” configurations. Its excitation energy is determined using 871.05 - 798.52 keV and 864.21 - 805.34 keV cascades, which are highlighted in green and red in Fig. 5.

The excitation energy of the first excited state was determined using energy differences between transitions feeding the ground state. The cascade of 60.37 - 173.96 - 730.93 - 704.33 keV feeding the first-excited state gives its initial excitation state 1682.30 keV (within experimental uncertainties). This cascade is highlighted by red lines in Fig. 6 and all these transitions except 60.37 keV are found in coincidence with each other, while 60.37 keV is clearly assigned to the  $^{183}\text{Hg}$  decay. The singles spectrum detected

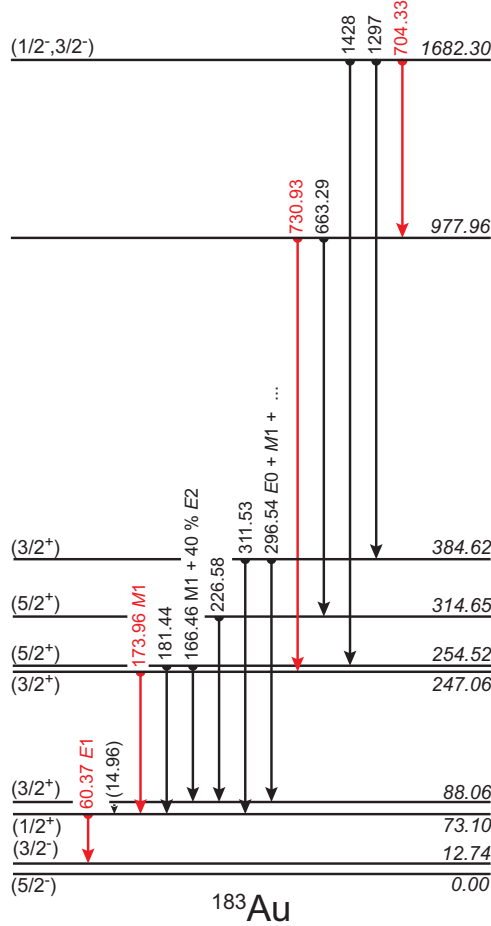


Figure 6: Partial level scheme of low-lying, positive-parity states associated with the  $3s_{1/2}$  and  $2d_{3/2}$  proton-hole configurations in the  $^{183}\text{Au}$  isotope deduced from the present work [7]. Transition energies were determined using the  $\gamma$ -ray singles spectrum detected with the BEGe detector. Transitions with energies given as integer numbers are either weak, dominated by other  $\gamma$  lines, or their energy exceeds 980 keV, which was the upper limit for the BEGe detector in this experiment, see the text for details. Their location in the scheme is proved by the  $\gamma$ - $\gamma$  coincidences. All states are populated via the decay of the 1682.30 keV state. Decay paths used for the localisation of the critical 60.73 keV transition connecting intruder and proton-hole states are highlighted in red colour.

with the Si(Li) detector was used to determine the multipolarity of the 60.37 keV transition. We assign the 60.37 keV as an  $E1$  transition with no abnormality and it was assigned as parity-changing  $1/2^+ \rightarrow 3/2^-$  transition, while the previous study [8] assigned the 60.37 keV transition as an “abnormal”  $E1$  transition.

Two transitions with mixed  $E0 + M1 + E2$  multipolarity reported in previous study [8] were observed in present data set with energies of 296.54 and 284.40 keV, see Fig. 3 and Fig. 4. Both transitions are highly converted due to their  $E0$  components, and therefore rather conversion electrons were used for coincidence analysis than  $\gamma$  rays due to the limited counting statistics of the present data set. The 296.54 keV transition was placed into the level scheme, see Fig. 5. However, no coincidences were observed for 284.40 keV transition due to the limited counting statistics of the present data set, and therefore it was not placed into the level scheme.

A number of incorrect features in the previous study of the  $^{183}\text{Hg} \rightarrow ^{183}\text{Au}$  decay scheme [8] has been discovered.

### $^{181}\text{Hg}$ decay

The half-life of  $^{181}\text{Hg}$  is 3.6(1) s [11] and the  $\beta$ -decay energy is 7210(25) keV [12].

Previously, the  $^{181}\text{Hg} \rightarrow ^{181}\text{Au}$  isotope was studied only at the ISOCELE facility [17] at Orsay. This experiment used a Pt-B alloy target placed inside of the ion source of ISOCELE mass separator. This target was irradiated either by 200 MeV proton or 270 MeV  $^3\text{He}$  beam delivered by Orsay synchrocyclotron with typical intensity of  $2 \mu\text{A}$ . Proton-beam irradiation produced  $^{181}\text{Au}$  activity, while  $^3\text{He}$ -beam irradiation a mixture of  $^{181}\text{Hg}$  and  $^{181}\text{Au}$  activities. Both datasets were strongly contaminated with  $^{181}\text{Pt}$ . Pure spectrum of  $^{181}\text{Au}$  was obtained by subtraction of proton- and  $^3\text{He}$ -beam data.

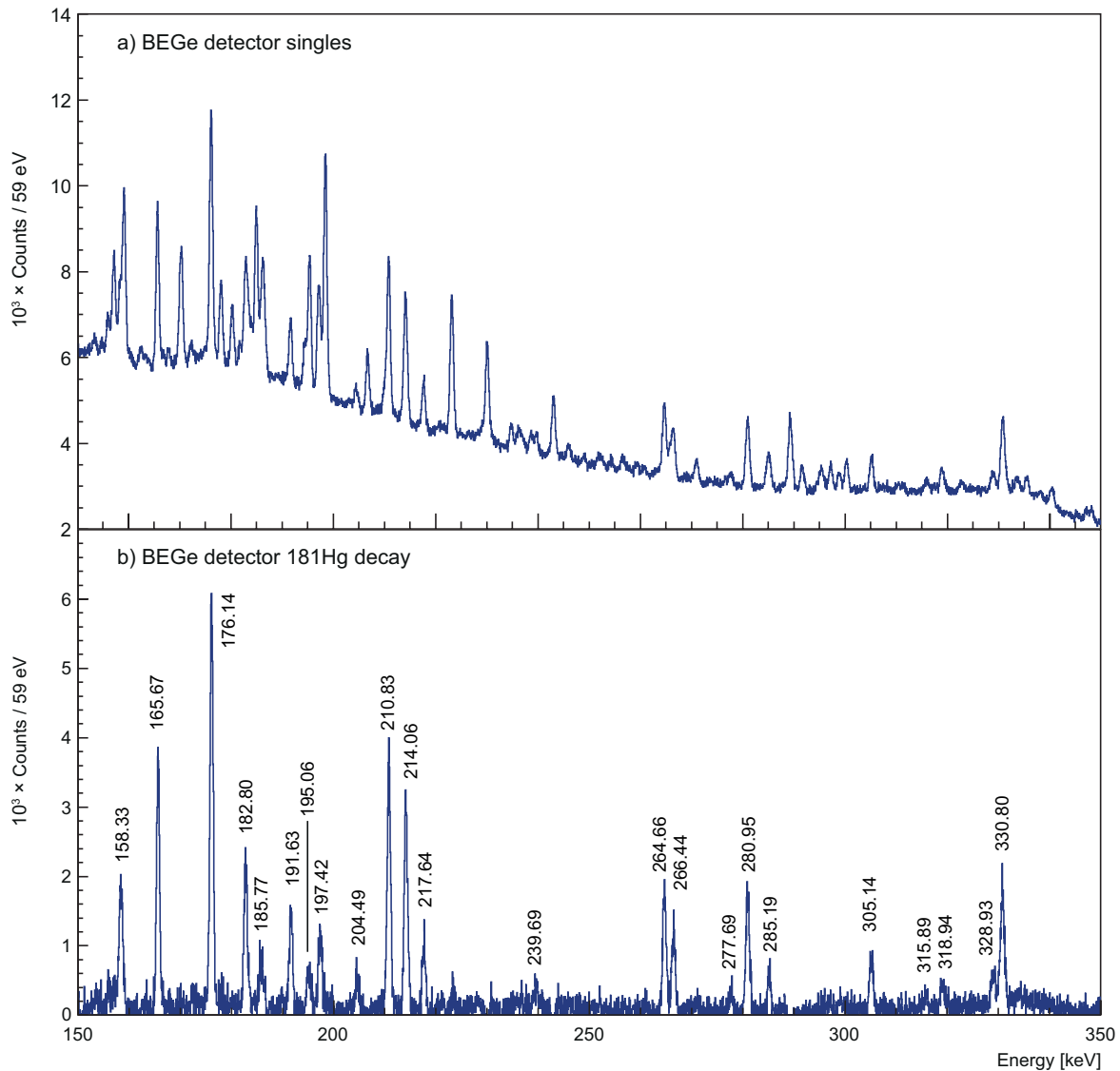


Figure 7: Part of singles  $\gamma$ -ray spectra measured with the BEGe detector. (a) is total singles spectrum and (b) is single spectrum assigned to the  $^{181}\text{Hg}$  decay.

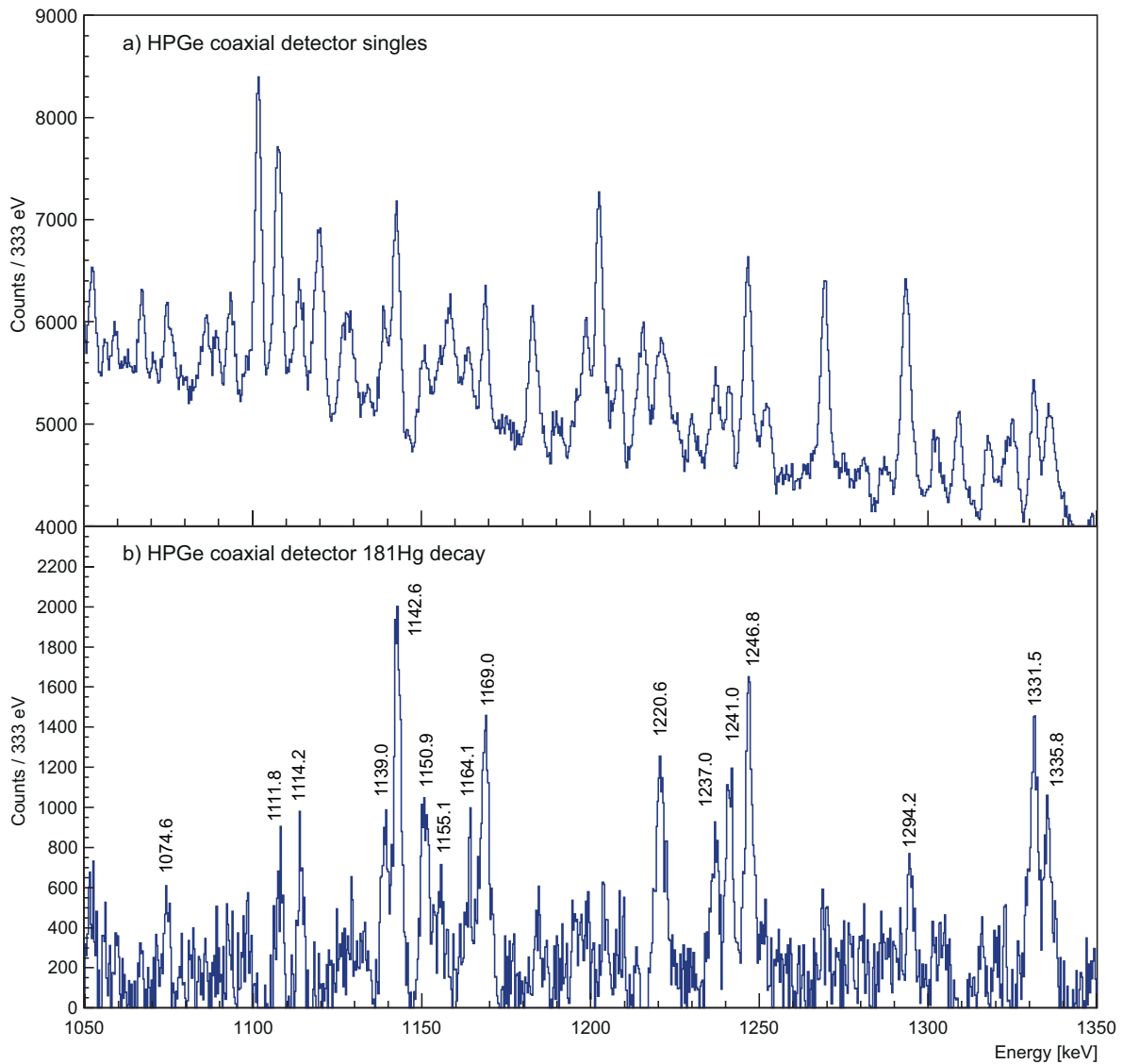


Figure 8: Part of singles  $\gamma$ -ray spectra measured with coaxial HPGe detector. (a) is total singles spectrum and (b) is single spectrum assigned to the  $^{181}\text{Hg}$  decay.

Resulting spectrum was still strongly contaminated with  $^{181}\text{Pt}$  transitions as it is explicitly stated by authors of the study [17]. No level scheme was constructed for  $^{181}\text{Hg}$ , only the table with  $\gamma$  rays is given in [17]. The only other literature relevant to the structure of the  $^{181}\text{Au}$  isotope are in-beam studies [18, 19].

Data for analysis of  $^{181}\text{Hg}$  were obtained during IS521 experiment in 2014 only. One BEGe and two coaxial HPGe detectors were employed. Innovative method for spectra separation was used and the comparison of total singles (a) and deconvoluted  $^{181}\text{Hg}$  decay singles spectra (b) measured with the BEGe detector is in Fig. 7 and measured with one of the coaxial HPGe detectors is in Fig. 8.

The level scheme of  $^{181}\text{Au}$  deduced from present work is given in Fig. 9. The level scheme construction is based on  $\gamma$ - $\gamma$ -ray coincidences in conjunction with Rydberg-Ritz combination principle. The spin and parity assignments are based on  $\gamma$ - $\gamma$ -ray coincidences and similarities in systematics of adjacent odd-Au isotopes. Only part of



The excitation energy of the first excited state was determined as weighted average of energy differences between couples of transitions feeding the ground state and the first excited state.

### Systematics of $1h_{11/2}$ proton-hole structure

In a comprehensive study of  $^{187}\text{Au}$  isotope [20], a rich spectrum (up to spin  $19/2^-$ ) of excited states associated with the  $1h_{11/2}$  proton-hole structure was observed. Two families of states were identified: either due to coupling of the  $1h_{11/2}$  proton hole with weakly deformed ground state, or with strongly deformed  $0^+$  intruder state in  $^{188}\text{Hg}$  core. To characterize these states, calculations with the particle + triaxial rotor model (PTRM) [23] using a Woods-Saxon potential for deformed mean field were performed in study [20]. Weakly deformed triaxial shape with  $\beta_2 = 0.15$  and  $\gamma = 32^\circ$  was used for description of states corresponding to coupling of the proton hole with ground state of  $^{188}\text{Hg}$ . In general, there is a good agreement between theory and experiment, and every state predicted by the calculation has its experimental counterpart, see Fig. 19 in [20]. Intensities of gamma rays connecting excited states of the  $1h_{11/2}$  structure were also calculated, see Tab. IV. in [20]. Overall the agreement is reasonably good, although some discrepancies clearly exist. The systematics has been extended to  $^{185}\text{Au}$  isotope [21, 22].

In present study, only  $3/2^-$ ,  $7/2^-$ , and  $11/2^-$  members of the  $1h_{11/2}$  proton-hole configuration could be identified in  $^{181,183}\text{Hg}$  isotopes. Only the low-spin isomer is present in  $^{181,183}\text{Hg}$ . This is not the case of heavier isotopes that have also  $13/2^+$  isomer, which decays via  $\beta^+$ /EC decay. Fig. 10 gives the systematics of the  $3/2^-$ ,  $7/2^-$ , and  $11/2^-$  states of the  $1h_{11/2}$  configuration together with  $9/2^-$  intruder state in odd-Au isotopes.

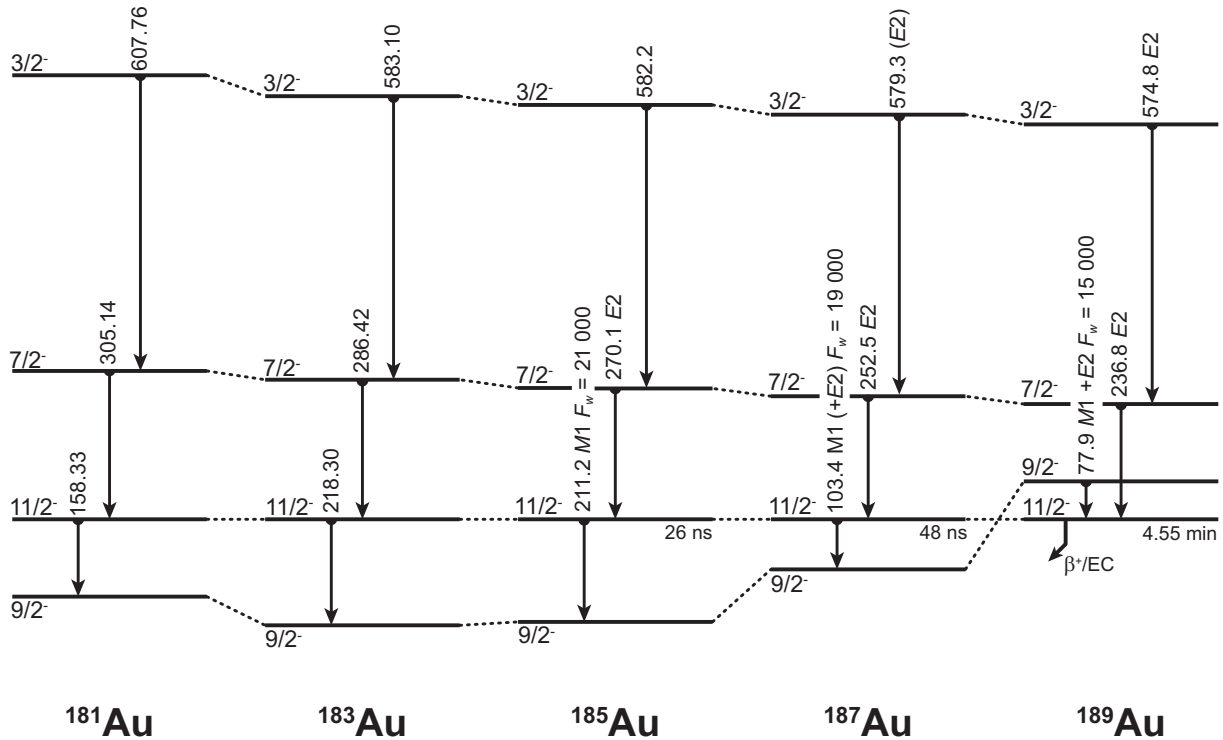


Figure 10: Systematics of the  $3/2^-$ ,  $7/2^-$ , and  $11/2^-$  states of the  $1h_{11/2}$  configuration together with  $9/2^-$  intruder state in odd-Au isotopes. The data are taken from present work and from [20–22].

$11/2^-$  states of the  $1h_{11/2}$  configuration together with  $9/2^-$  intruder state, which is the final state of the deexcitation of  $11/2^-$  band head (fed by retarded  $M1$  transition).

The excitation energy of  $3/2^-$  and  $7/2^-$ , relative to the  $11/2^-$  band head appears to be notably stable, suggesting very similar structure as was established in  $^{187}\text{Au}$  by authors of study [20]. However, there is slight increase in split of  $3/2^-$  and  $7/2^-$  states. The same trend is observed also in the systematics of these states in heavier Au isotopes [24]. According to calculations using PTRM model, this indicates a slight change in the triaxiality from “oblatish” to “prolatish” shape with decreasing neutron number.

### Systematics of $2d_{3/2} \oplus 3s_{1/2}$ proton-hole configuration

Fig. 11 gives the systematics of positive-states associated with mixed  $2d_{3/2} \oplus 3s_{1/2}$  proton-hole configuration in  $^{183,185,187,189}\text{Au}$  isotopes. The data are from present work ( $^{183}\text{Au}$ ) and from [20, 21, 25]. Sequence of states is markedly similar through given isotopes. However, the states are more compressed with decreasing neutron number. This can be explained by presence of low-spin intruder states, which appear due to coupling of proton hole with coexisting  $0^+$  states in even-Hg cores. Mixing repulsion between the states with the same spin-parity may cause the compression in isotopes close to  $N = 104$  midshell point.

Electric monopole transition was identified between  $3/2^+$  states in  $^{183}\text{Au}$ . This is probably deexcitation of one of above mentioned positive-parity intruder configurations.

Calculations on the basis of the PTRM model, performed for  $^{187}\text{Au}$  in [20], suggest slightly deformed triaxial configuration with  $\beta_2 = 0.15$  and  $\gamma = 45^\circ$ . A discrepancy be-

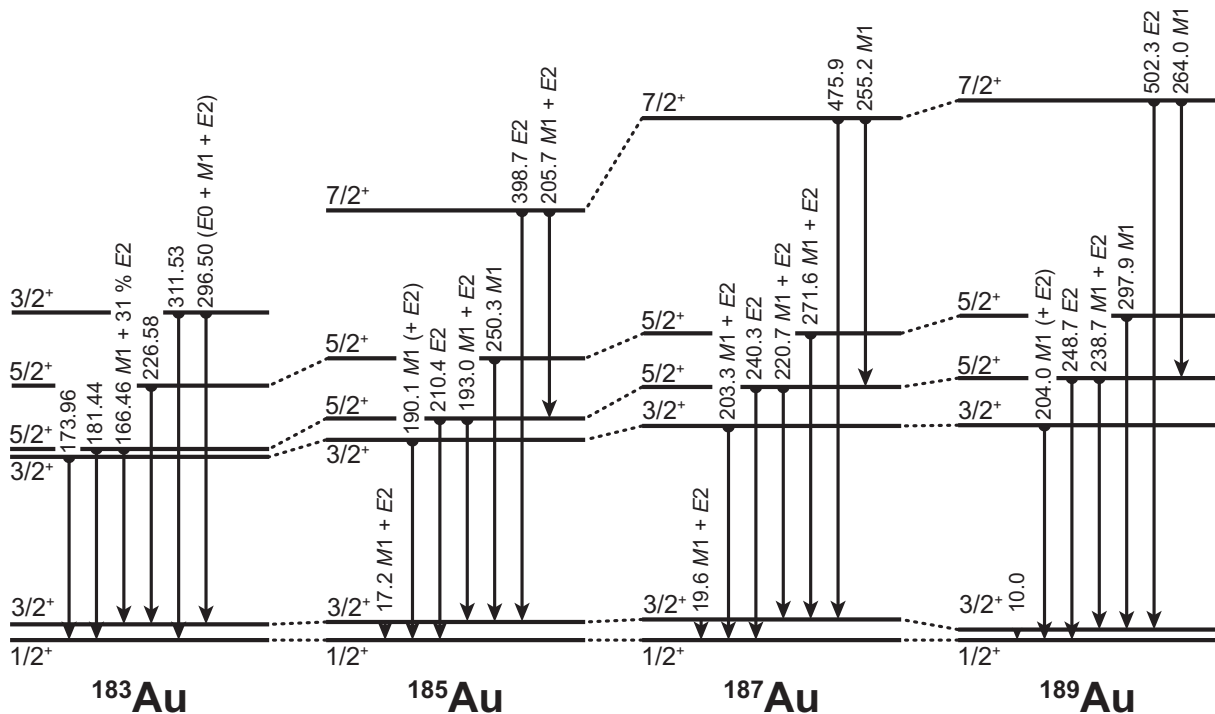


Figure 11: Systematics of positive-parity states of  $2d_{3/2} \oplus 3s_{1/2}$  proton-hole configurations in odd-Au isotopes. The data are taken from present work ( $^{183}\text{Au}$ ) and from [20, 21, 25].



tween gamma deformation obtained for  $1h_{11/2}$ , may be caused by mixing that affects the states associated with  $2d_{3/2} \oplus 3s_{1/2}$  configuration more than those associated with  $1h_{11/2}$  configuration. That is an unique-parity orbital and thus is very pure configuration.

In  $^{181}\text{Au}$  isotope, no coincidences were observed for candidates for positive states, due to lack of the statistics, and therefore they cannot be assigned into the level scheme. Thus, new spectroscopy investigation of  $^{181}\text{Au}$  isotope is highly demanding. This must involve detection of conversion electrons, including low energies.

### Systematics of intruder configurations

The key result of the IS521 experiment is shown in Fig. 12. It gives a systematics of  $3/2^-$ ,  $5/2^-$ ,  $7/2^-$ , and  $9/2^-$  states associated with intruder configurations, depicted relatively to  $1/2^+$ , and  $3/2^+$  states of “normal” configuration. It reveals parabolic trend, which emerges to be a general characteristic of intruder configurations [2]. Minimum is located at  $N = 104$ , i.e., exactly in the midshell point.

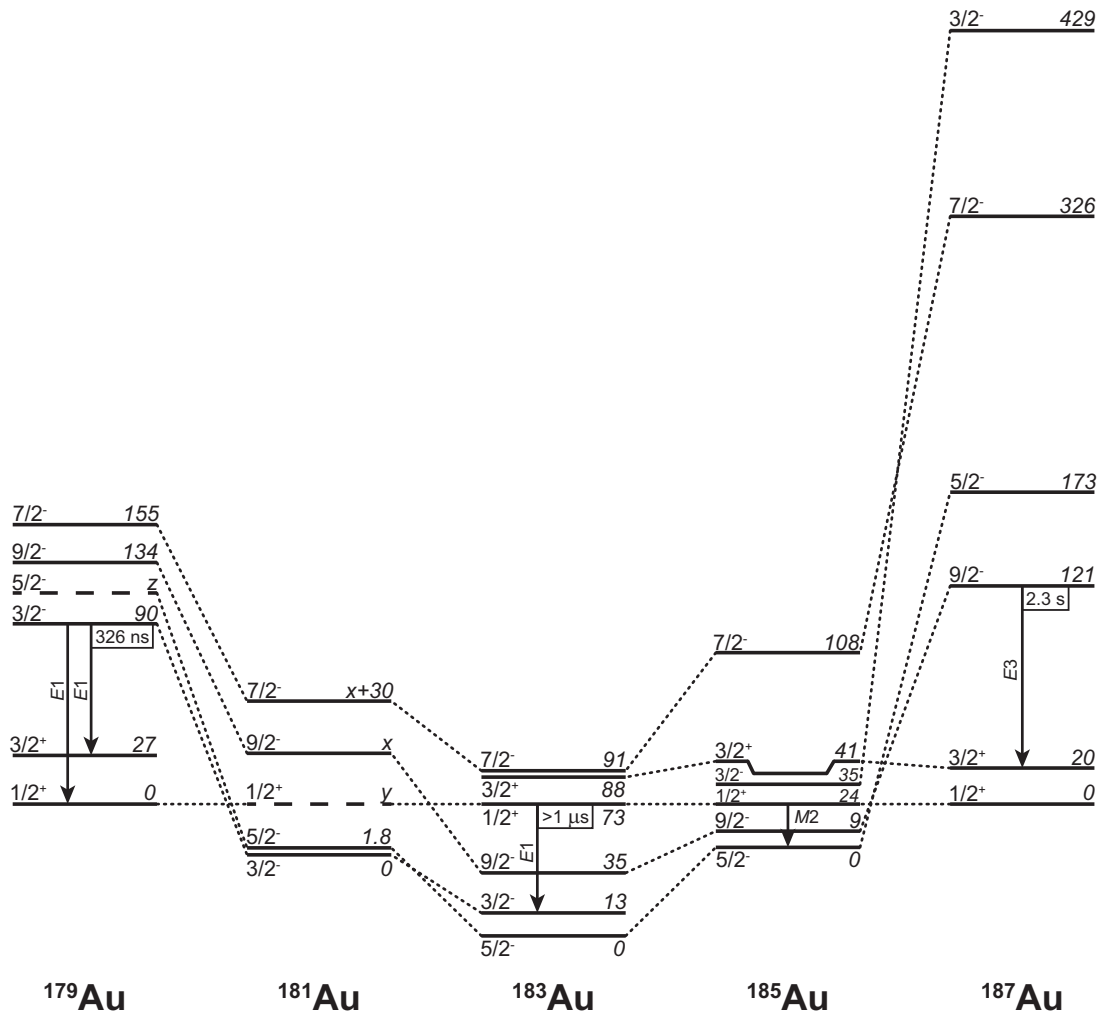


Figure 12: Systematics of  $3/2^-$ ,  $5/2^-$ ,  $7/2^-$ , and  $9/2^-$  states associated with intruder configurations, depicted relatively to  $1/2^+$ , and  $3/2^+$  states associated with  $2d_{3/2} \oplus 3s_{1/2}$  proton-hole configurations in odd-Au isotopes. The data are taken from this work and from [20, 21, 25, 26]

## References

- [1] E. Rutherford. "The scattering of  $\alpha$  and  $\beta$  particles by matter and the structure of the atom". In: *The London, Edinburgh, and Dublin Philosophical Magazine and Journal of Science* 21 (1911), pp. 669–688. DOI: 10.1080/14786440508637080.
- [2] K. Heyde and J. L. Wood. "Shape coexistence in atomic nuclei". In: *Reviews of Modern Physics* 83 (2011), pp. 1467–1521. DOI: 10.1103/RevModPhys.83.1467.
- [3] J. L. Wood et al. "Coexistence in even-mass nuclei". In: *Physics Reports* 215 (1992), pp. 101–201. DOI: 10.1016/0370-1573(92)90095-H.
- [4] K. Heyde et al. "Coexistence in odd-mass nuclei". In: *Physics Reports* 102 (1983), pp. 291–393. DOI: 10.1016/0370-1573(83)90085-6.
- [5] M. Venhart et al. "Simultaneous spectroscopy of  $\gamma$  rays and conversion electrons: Systematic study of E0 transitions and intruder states in close vicinity of mid-shell point in odd-Au isotopes". In: *CERN-INTC* 302 (Jan. 2011), pp. 1–10. URL: <http://cds.cern.ch/record/1319317/files/INTC-P-302.pdf?version=2>.
- [6] W. Ritz. "On a New Law of Series Spectra". In: *Astronomical Journal* 28 (1908), pp. 237–243. DOI: 10.1086/141591.
- [7] M Venhart et al. "New systematic features in the neutron-deficient Au isotopes". In: *Journal of Physics G: Nuclear and Particle Physics* 44 (2017), p. 074003. DOI: 10.1088/1361-6471/aa7297.
- [8] M.I. Macias-Marques et al. "Decays of  $^{183}\text{Hg}$  and  $^{183}\text{Au}$ ". In: *Nuclear Physics A* 427 (1984), pp. 205–223. DOI: 10.1016/0375-9474(84)90082-4.
- [9] V. Matoušek et al. "TATRA: a versatile high-vacuum tape transportation system for decay studies at radioactive-ion beam facilities". In: *Nuclear Instruments and Methods in Physics Research Section A: Accelerators, Spectrometers, Detectors and Associated Equipment* 812 (2016), pp. 118–121. DOI: 10.1016/j.nima.2015.12.039.
- [10] M. Venhart et al. "Application of the Broad Energy Germanium detector: A technique for elucidating  $\beta$ -decay schemes which involve daughter nuclei with very low energy excited states". In: *Nuclear Instruments and Methods in Physics Research Section A: Accelerators, Spectrometers, Detectors and Associated Equipment* 849 (2017), pp. 112–118. DOI: 10.1016/j.nima.2016.12.048.
- [11] J.K. Tuli. *Current Version of Nuclear Wallet Cards*. 2017. URL: <https://www.nndc.bnl.gov/wallet/wccurrent.html> (visited on 02/20/2019).
- [12] M. Wang et al. "The Ame2012 atomic mass evaluation". In: *Chinese Physics C* 36 (2012), pp. 1603–2014. DOI: 10.1088/1674-1137/36/12/003.
- [13] P. Hornshøj et al. "Beta-strength functions of neutron-deficient isotopes in the xenon and mercury regions". In: *Nuclear Physics A* 239 (1975), pp. 15–28. DOI: 10.1016/0375-9474(75)91130-6.
- [14] J. Bonn et al. "Spins, moments and charge radii in the isotopic series  $^{181}\text{Hg}$ – $^{191}\text{Hg}$ ". In: *Zeitschrift für Physik A Atoms and Nuclei* 276 (1976), pp. 203–217. DOI: 10.1007/BF01412098.

- [15] U. Krönert et al. "Observation of strongly deformed ground-state configurations in  $^{184}\text{Au}$  and  $^{183}\text{Au}$  by laser spectroscopy". In: *Zeitschrift für Physik A: Atomic Nuclei* 331 (1988), pp. 521–522. DOI: 10.1007/BF01291911.
- [16] T. Kibédi et al. "Evaluation of theoretical conversion coefficients using BrIcc". In: *Nuclear Instruments and Methods in Physics Research Section A: Accelerators, Spectrometers, Detectors and Associated Equipment* 589 (2008), pp. 202–229. DOI: 10.1016/j.nima.2008.02.051.
- [17] J. Sauvage et al. "Decays of  $^{181}\text{Hg}$  ( $T_{1/2} = 3.6$  s) and  $^{181}\text{Au}$  ( $T_{1/2} = 11.4$  s), and low-spin states of  $^{181}\text{Pt}$  and  $^{177,181}\text{Ir}$ ". In: *Nuclear Physics A* 540 (1992), pp. 83–116. DOI: 10.1016/0375-9474(92)90196-Q.
- [18] W. F. Mueller et al. "High-spin structure in  $^{181,183}\text{Au}$ ". In: *Physical Review C* 59 (1999), pp. 2009–2032. DOI: 10.1103/PhysRevC.59.2009.
- [19] L. T. Song et al. "High-spin level scheme of  $^{183}\text{Au}$ ". In: *Physical Review C* 71 (2005), p. 017302. DOI: 10.1103/PhysRevC.71.017302.
- [20] D. Rupnik et al. "Levels of  $^{187}\text{Au}$ : A detailed study of shape coexistence in an odd-mass nucleus". In: *Physical Review C* 58 (1998), pp. 771–795. DOI: 10.1103/PhysRevC.58.771.
- [21] M. O. Kortelahti et al. "Nuclear systematics far from the line of beta stability: the low-lying excited states of  $^{185,187,189}\text{Au}$ ". In: *Journal of Physics G: Nuclear Physics* 14.11 (1988), p. 1361. URL: <https://iopscience.iop.org/article/10.1088/0305-4616/14/11/008/meta>.
- [22] C. D. Papanicolopoulos. "Shape Coexistence in Odd-Mass Nuclei Near  $Z = 82$  Closed Shell: A Study of the Excited States of  $^{185}\text{Au}$  in the  $\beta^+$ /EC Decay of  $^{185}\text{Au}$ ." PhD thesis. Georgia Institute of Technology, 1987.
- [23] S. E. Larsson, G. Leander, and I. Ragnarsson. "Nuclear core-quasiparticle coupling". In: *Nuclear Physics A* 307 (1978), pp. 189–223. DOI: 10.1016/0375-9474(78)90613-9.
- [24] E. F. Zganjar et al. "Rotation-aligned coupling and axial asymmetry in  $^{189-195}\text{Au}$ ". In: *Physics Letters B* 58 (1975), pp. 159–162. DOI: 10.1016/0370-2693(75)90627-9.
- [25] J. L. Wood et al. "Decay of mass-separated  $^{189m}\text{Hg}$  (8.7 min) and  $^{189g}\text{Hg}$  (7.7 min) to  $^{189}\text{Au}$ ". In: *Nuclear Physics A* 600 (1996), pp. 283–334. DOI: 10.1016/0375-9474(95)00478-5.
- [26] M. Venhart et al. "Shape coexistence in odd-mass Au isotopes: Determination of the excitation energy of the lowest intruder state in  $^{179}\text{Au}$ ". In: *Physics Letters B* 695 (2011), pp. 82–87. DOI: 10.1016/j.physletb.2010.10.055.

## List of publications

2017

M. Venhart, J. L. Wood, A. J. Boston, T. E. Cocolios, L. J. Harkness-Brennan, R. D. Herzberg, D. T. Joss, D. S. Judson, J. Kliman, V. Matoušek, Š. Motyčák, R. D. Page, A. Patel, K. Petřík, M. Sedlák, M. Veselský.

*“Application of the Broad Energy Germanium detector: A technique for elucidating decay schemes which involve daughter nuclei with very low energy excited states”.*

Nuclear Instruments and Methods in Physics Research Section A **849**, 112–118 (2017).

M. Venhart, J. L. Wood, M. Sedlák, M. Balogh, M. Bírová, A. J. Boston, T. E. Cocolios, L. J. Harkness-Brennan, R.-D. Herzberg, L. Holub, D. T. Joss, D. S. Judson, J. Kliman, J. Klimo, L. Krupa, J. Luštnák, L. Makhathini, V. Matoušek, Š. Motyčák, R. D. Page, A. Patel, K. Petřík, A. V. Podshibyakin, P. M. Prajapati, A. M. Rodin, A. Špaček, R. Urban, C. Unsworth, M. Veselský.

*“New systematic features in the neutron-deficient Au isotopes”.*

Journal of Physics G: Nuclear and Particle Physics **44**, 074003 (2017).

M. Venhart, F. A. Ali, W. Ryssens, J. L. Wood, D. T. Joss, A. N. Andreyev, K. Auranen, B. Bally, M. Balogh, M. Bender, R. J. Carroll, J. L. Easton, P. T. Greenlees, T. Grahn, P.-H. Heenen, A. Herzáň, U. Jakobsson, R. Julin, S. Juutinen, D. Klíč, J. Konki, E. Lawrie, M. Leino, V. Matoušek, C. G. McPeake, D. O’Donnell, R. D. Page, J. Pakarinen, J. Partanen, P. Peura, P. Rahkila, P. Ruotsalainen, M. Sandzelius, J. Sarén, B. Saygi, M. Sedlák, C. Scholey, J. Sorri, S. Stolze, A. Thornthwaite, J. Uusitalo, M. Veselský.

*“De-excitation of the strongly coupled band in  $^{177}\text{Au}$  and implications for core intruder configurations in the light Hg isotopes”.*

Physical Review C **95**, 061302(R) (2017).

2016

V. Matoušek, M. Sedlák, M. Venhart, D. Janičkovič, J. Kliman, K. Petřík, P. Švec, P. Švec, Sr., M. Veselský.

*“TATRA: a versatile high-vacuum tape transportation system for decay studies at radioactive-ion beam facilities”.*

Nuclear Instruments and Methods in Physics Research Section A **812**, 118–121 (2016).